A 0.45NW, 0.5V, 59-DB DR, G_M-C LOW-PASS FILTER FOR PORTABLE ECG RECORDING

Chutham Sawigun, Senad Hiseni and Wouter A. Serdijn
Biomedical Electronics Group, Electronics Laboratory, Delft University of Technology, Mekelweg 4, 2628 CD, Delft, The Netherlands

Keywords: Analog Circuit, G_m-C Filter, Low-Pass Filter, Sub-Threshold CMOS, Ultra Low-Power, Weak Inversion.

Abstract: This paper presents the design of a sub-threshold CMOS G_m-C low-pass filter in a portable ECG detection system. The proposed filter is formed by cascading 6 stages of identical 1st-order low-pass sections. With a minimum number of active components in the 1st-order section, the noise contribution of the circuit can be kept low while minimizing the size of transistors and capacitors. The filter cut-off frequency is designed to be adjustable over the range from 100Hz to 250Hz by changing the bias current. Circuit simulations, using AMS' 0.18µm CMOS technology and operating from a 0.5V supply voltage, show that, for a cut-off frequency of 150Hz, the filter draws 0.9nA of current. An input referred noise of 88µV_{rms} is obtained while for 1% total harmonic distortion, the voltage swing can be as high as 0.23Vpp.

1 INTRODUCTION

As a consequence of the heart activity, electrocardiograms (ECGs) can be recorded by skin electrodes (Webster, 1995). By measuring the ECG signal, the heart condition can be diagnosed and monitored. In a portable ECG detection system a low-pass filter (LPF) is required to impede high frequency electrical signals from non-cardiac muscles (muscle noise or artifact) (Garcia-Niebla and Serra-Autonell, 2009) and to avoid aliasing in the sampling process of an analog to digital converter (ADC) (Lee and Cheng, 2009).

In order to minimize power consumption of the LPF in the portable ECG detector, weak inversion operation of CMOS devices is the first condition to handle for a design using very little bias current. Nonlinearity, noise and mismatch of this operating region are, however, more severe than that of its strong inversion counterpart. Recently, the systematic design of an ECG filter optimizing those non-idealities within a linearized G_m-C filter structure has been reported (Lee and Cheng, 2009). A very good figure-of-merit (FoM) was obtained at a power consumption of only 453nW.

To further reduce the power consumption, this paper proposes a LPF design technique that does not require a linear G_m. Instead of trying to linearize the G_m cell to obtain a good performance before substituting it into a passive prototype LC filter, a nonlinear G_m with feedback is used to create a 1st-order LPF cell before forming the higher order filter by cascading the identical 1st-order cells. This approach can reduce a lot of power while other performances remain the same (or become even better) in the pass-band of the LPF. To demonstrate this idea, we exploit a follower integrator (FI) (Mead, 1989) as the fundamental element of our ECG filter, which subsequently is realized by cascading 6 FI stages. Simulation results, using Cadence with AMS' 0.18µm CMOS model parameters, confirm that for comparable performance, the proposed ECG filter's power consumption is three orders of magnitude lower than that of the LPF in (Lee and Cheng, 2009).

The remaining sections of the paper are organized as follows. In Sec. II, a brief description of the ECG portable detector is shown. The basic concept of the 1st-order FI based filter is described and a 6th-order Bessel LPF is presented in Sec. III. Next, Sec. IV presents the simulation results. The conclusions will be drawn in the last section.

2 LOW-PASS FILTER DESIGN ISSUES IN ECG DETECTOR

Fig. 1 illustrates a portable ECG detection device.

Sawigun C., Hiseni S. and A. Serdijn W..
A 0.45NW, 0.5V, 59-DB DR, GM-C LOW-PASS FILTER FOR PORTABLE ECG RECORDING.
DOI: 10.5220/0003764103240328
In *Proceedings of the International Conference on Biomedical Electronics and Devices* (BIODEVICES-2012), pages 324-328
ISBN: 978-989-8425-91-1
Copyright © 2012 SCITEPRESS (Science and Technology Publications, Lda.)

First, a low noise amplifier is used to amplify the very weak ECG signal. Depending on the electrodes used, ECG signal amplitudes can range from around 50µV to approximately 4 mV (see Fig. 2) (Webster, 1995). Next, high frequency components of the ECG signal are filtered out to decrease the out-of-band noise. Herein, the recommended low-pass cut off

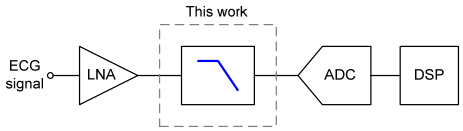

Figure 1: Portable ECG detection.

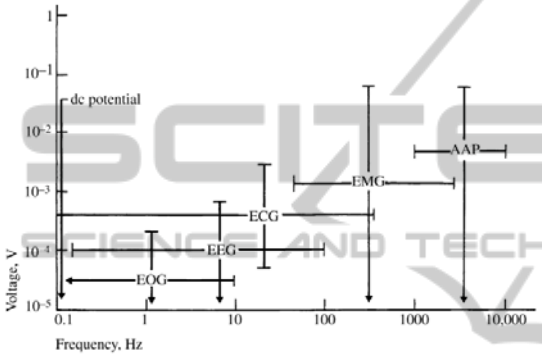

Figure 2: Different biopotential voltages versus frequency spectrum (Webster, 1995).

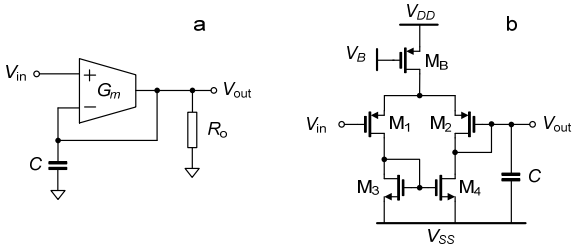

Figure 3: Follower integrator a) macro-model b) transistor level circuit.

frequencies are 150Hz and 250Hz in case of adults and children, respectively (Kligfield et al., 2007) (Rijnbeek et al., 2001). Afterwards, an ADC is utilized in which the analog input signal is quantized and converted into digital values as needed for the subsequent digital signal processing (DSP).

Since there is a large variation on the expected amplitude of the input signal, the amplifier and filter are required to have a minimal Dynamic Range (DR), according to (Lee and Cheng, 2009) (Luo and Johnston, 2010), of

$$DR = 20\log\left(\frac{2ECG_{\max}}{ECG_{\min}}\right) \cong 44\text{dB}\,. \qquad (1)$$

To avoid aliasing, the filter should provide sufficient attenuation in the stop-band. In (Lee and Cheng, 2009), for a sampling frequency (f_s) of 1kS/s, 29dB attenuation at 500Hz (f_s/2) was found. In this work, we target the same numbers of attenuation and sampling rate. Besides, to minimize phase distortion, a constant group delay over the pass-band response of the filter should be obtained (Hejjel and Kellenyi, 2005).

3 FOLLOWER INTEGRATOR BASED LOW-PASS FILTER

The FI is conceptually shown in Fig. 3a. It comprises a transconductor and a grounded capacitor connected in a negative-feedback fashion. Resistor R_o represents the output resistance of the transconductor to ground (which is usually many times larger than G_m^{-1}). We then find that

$$\frac{V_{\text{out}}(s)}{V_{\text{in}}(s)} = \left(\frac{G_m R_o}{1+G_m R_o}\right)\frac{1}{\left(1+\frac{sCR_o}{1+G_m R_o}\right)} \cong \frac{1}{1+s\frac{C}{G_m}}\,. \qquad (2)$$

As one can see from (2), the FI provides a low-pass frequency response with a pass-band gain and cut-off frequency of $K \cong 1$ and $f_c = G_m/2\pi C$, repectively.

According to this characteristic, V_{out} is following V_{in} closely for input signal frequencies below f_c. In other words, the differential input voltage of the G_m is kept small, which helps the filter to suffer less from nonlinearity of the G_m itself. Benefitting from the fact mentioned above, high dynamic range low-pass filters realized from nonlinearized G_ms have been successfully implemented in (Python, 1999) and (D'Amico et al., 2006). Hence, without linearization, the G_ms can be made compact and low noise and low-power consumption can be expected while a good linearity can be achieved due to the large loop-gain at low frequencies.

The FI can be simply formed by the circuit shown in Fig. 3b (Mead, 1989). It comprises a simple differential pair M1-M2 biased by current source MB with a current mirror active load, M3-M4, and a grounded capacitor, C.

Neglecting channel length modulation, the capacitance current can be found to be

$$I_C = I_B \tanh\left(\frac{V_{\text{in}} - V_{\text{out}}}{2nU_T}\right). \qquad (3)$$

The nonlinear relation in (3) is shown here to give

an intuitive understanding that at low frequencies $I_C \cong 0$ and consequently, V_{in} and V_{out} are forced to be equal. The hyperbolic tangent function will not produce any distortion in this case. But for higher frequencies, the phase difference between $V_{in} \cong V_{out}$ becomes greater and more distortion will be produced.

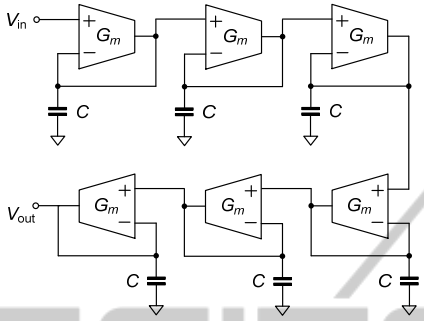

Figure 4: FI based 6th order LPF.

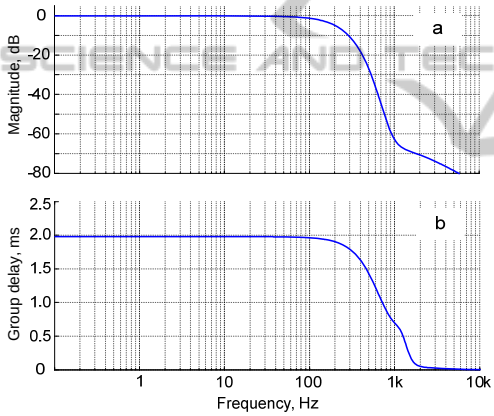

Figure 5: Frequency response of the proposed filter a) magnitude response b) group delay.

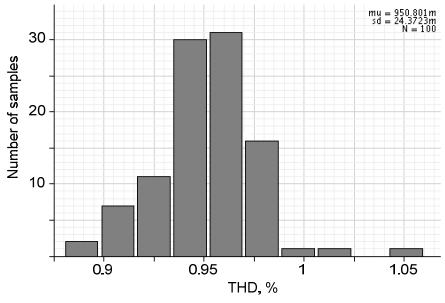

Figure 6: Monte-Carlo simulation.

The power spectral density of the output noise voltage can be found to be (at low frequencies)

$$S_{vno}(f) = \frac{8nkT}{G_m} + \frac{2K_F}{C_{OX} f}\left(\frac{1}{WL_1} + \frac{1}{WL_3}\right), \qquad (4)$$

where K_F is a flicker noise parameter, all the other symbols have their usual meanings, $WL_1 = WL_2$, $WL_3 = WL_4$ and $G_m = I_B/2nU_T$.

For our application that deals with input frequencies below a few hundred hertz, the majority of the noise power is not only contributed by the thermal noise but also by $1/f$ noise. From (4) the noise corner frequency can be found as

$$f_{corner} = \frac{qI_B K_F}{8(nkT)^2 C_{OX}\left(\frac{1}{WL_1} + \frac{1}{WL_3}\right)}. \qquad (5)$$

We can see from (5) that to keep f_{corner} low, the FI requires large transistor sizes and low bias current.

The requirements of the filter mentioned in Section II can be simply met by cascading 6 identical FI stages as shown in Fig. 4. Formed by identical circuit elements this structure provides a Bessel transfer function. All the G_ms are realized by the transconductor in Fig. 3b. The advantages of this filter topology are pointed out in the following list:

- As a consequence of the use of identical components in a modular structure, the filter's sensitivity to capacitance and transconductance variations is low.
- The linearity of the filter is less susceptible to mismatch due to the unity gain feedback in each 1st-order section.
- The internal node voltage swings are all identical in the pass-band. Hence, the filter distortionless output swing is maximized (Groenewold, 1992).
- The contributions of all G_m stages to the overall output noise are almost equal. Hence, the filter output noise is minimized (Groenewold, 1992).
- Constant group delay can be expected in the pass-band frequency range.

The drawback is that the transition band roll-off is less steep compared to other filter types.

For a cutoff frequency of 150Hz, realizing this filter circuit within an acceptable chip area and obtaining very low power consumption to achieve a pass-band gain of 0dB and sufficient magnitude attenuation at $f_s/2$ = 500Hz are feasible.

4 CIRCUIT SIMULATIONS

The LPF circuit has been designed to be

implemented in AMS' 0.18μm CMOS process technology. The bias current of each FI circuit is set to I_B = 0.15nA. The total bias current for the filter core equals 0.9nA. Operated from a 0.5V supply, this results in 0.45nW static power. Dimensions of the MOS transistors used are listed in Table. I. The transistors are largely sized to reduce the transistor's flicker noise and mismatch. The total capacitance equals 6pF (1pF per stage).

Table 1: Transistor Dimensions.

MOSFET	W [μm]	L [μm]
M_1, M_2:M_3, M_4: M_B	15:8:12	2.5:8:6

Table 2: Performance Summary and Comparison.

	Lee and Cheng, 2009 (Measurement)	This work (Simulation)
Approx. type	Butterworth	Bessel
CMOS Tech.	0.18μm	0.18μm
V_{DD}	1V	0.5V
P	453nW	0.45nW
order, N	5	6
Total cap.	5.76pF	6pF
Pass-band gain	–10.5dB	0dB
f_{-3dB}	250Hz	150Hz
$f_s/2$ attenuation	–29dB*	–28dB
IRN	340μV_{rms}	88μV_{rms}
DR@THD (50Hz f_{in})	40.3dB@-48.6dB	59.3dB@-40dB, 52.1dB@-48.4dB
FoM	8.99×10^{-12} J	8.43×10^{-15} J, 9.6×10^{-15} J

* From the simulated frequency response

Fig. 5 shows the simulated magnitude response and the group delay of the proposed filter. The f_{-3dB} cut-off frequency is found at 150Hz and a magnitude attenuation of –28dB is obtained at 500Hz. The group delay of 2ms remains constant over the range of DC to 100Hz. At 250Hz a 0.6ms delay deviation from 2ms is found.

For a more realistic estimation of the circuit linearity, we also performed a statistical analysis. The effect of transistor mismatch is verified through a Monte-Carlo simulation for the condition of a 0.11V input amplitude. For 100 runs, the obtained result is very satisfying as can be seen from the histogram in Fig. 6. The mean value of the THD obtained is 0.95% with a standard deviation of 0.024%.

Table II shows a performance comparison between the proposed LPF and the measured results from the recently reported ECG LPF (Lee and Cheng, 2009) that relies on a linearized G_m composed of several transistors and a filter structure that does not contain local unity-gain feedback loops. Hence, high amounts of noise and mismatch induced nonlinearity cannot be avoided. Due to the compact G_m circuit and the local negative feedback in the FI structure, our proposed filter outperforms the previous ECG filter on most of its performance except the transition band attenuation and the value of the capacitance while the power consumption of our design is 1000 times lower. Considering the FoM (Vittoz and Tsividis, 2002) defined by $P\times\left(N\times f_{-3dB}\times DR\right)^{-1}$, where, N is the filter order and P is the power consumption, the proposed LPF also improves the FoM by approximately three orders of magnitude.

5 CONCLUSIONS

The design of a 6th-order G_m-C low-pass filter using nonlinear CMOS transconductors operating in their sub-threshold region has been presented. The presented filter features good linearity in the pass-band and mismatch insensitivity due to its embedded negative feedback within each fundamental FI cell. Low noise and low-power consumption are achieved from the compactness of the ordinary transconductors that we employ. The obtained simulation results confirm that our design fits portable ECG detection requirements well.

REFERENCES

D'Amico S., Conta M., Baschirotto A. 2006. A 4.1mW 10MHz fourth-order source-follower-based continuous-time filter with 79-dB DR, *IEEE J. Solid-State Circuits*, pp. 2713-2719.

Garcia-Niebla J., Serra-Autonell G., 2009. Effects of inadequate low-pass filter application, *Journal of Electrocardiography*, vol. 42, pp. 303-304.

Groenewold G., 1992, Optimal dynamic range integrators, *IEEE Trans. Circuits Syst. I*, vol. 39, p.614 .

Hejjel L., Kellenyi L., 2005. The corner frequencies of the ECG amplifier for heart rate variability analysis, *Physiological Measurement*, vol. 26, pp. 39–47.

Kligfield P., Gettes L. S., Bailey J. J., et al., 2007. Recommendations for the standardization and interpretation of the electrocardiogram, *J. Am. Coll Cardiol*, vol. 49, no. 10, pp 1109–1127.

Lee S. Y., Cheng C. J., 2009. Systematic design and modeling of a OTA-C filter for portable ECG detection, *IEEE Trans. Biomed. Circuits Syst.*, vol. 3, no. 1, pp. 53-64.

Luo S., Johnston P., 2010. A review of electrocardiogram filtering, *Journal of Electrocardiology*, vol. 43, no 6, pp 486 – 496.

SCITEPRESS SCIENCE AND TECHNOLOGY PUBLICATIONS

Mead C. A., 1989 *Analog VLSI and Neural Systems*. Addison-Wesley Publishing Co., Reading, MA, 1989.

Python D., Porret A. S., Enz C., 1999. A 1V 5th-order Bessel filter dedicated to digital standard proceses, *Proc. IEEE CICC*, pp. 505-508.

Rijnbeek P. R., Kors J. A., 2001. Witsenburg M., Minimum bandwidth requirements for recording of pediatric electrocardiograms, *Circulation*, vol. 104, pp 3087-3090.

Vittoz E., Tsividis Y., 2002 Frequency-dynamic range-power, in *Trade-Offs in Analog Circuit Design*, C. Toumazou, G. S. Moschytz, and B. Gilbert, Eds. Boston, MA: Kluwer, ch. 10.

Webster, J. G., 1995. *Medical Instrumentations: Application and Design*, New York: Wiley.

SCITEPRESS
SCIENCE AND TECHNOLOGY PUBLICATIONS